

## FUNCTIONALIZATION AND CROSS-LINKING OF CARBOXYMETHYL CELLULOSE IN AQUEOUS MEDIA

SAWSAN DACRORY,\* HUSSEIN ABOU-YOUSEF,\* SAMIR KAMEL,\* RAGAB E. ABOU-ZEID,\*  
MOHAMED S. ABDEL-AZIZ\*\* and MOHAMED ELBADRY\*\*\*

\*Cellulose and Paper Department, National Research Centre, Egypt

\*Microbial Chemistry Department, National Research Centre, Egypt

\*\*\*Department of Chemistry, Faculty of Science, Ain Shams University, Abasia, Egypt

✉ Corresponding author: Sawsan Dacrory, sawsannrc2012@yahoo.com

Received October 13, 2017

Lignocelluloses are the main components of the wastes of olive oil industrial production. Partially destoned olive wastes contain a small amount of oil and water. So, olive wastes should have lower fiber content in comparison with crude olive waste. Functionalization of cellulose extracted from olive wastes enhances its importance for production of antimicrobial materials. In this work, dialdehyde carboxymethyl cellulose (DCMC), as cross-linking agent, was successfully prepared by using periodate oxidation of carboxymethyl cellulose (CMC), which had been previously prepared from olive oil by-products. CMC was modified with hydrazine monohydrate in order to prepare carboxymethyl hydrazide (NCCM), which was reacted with DCMC through Schiff's base reaction, resulting in cross-linking of NCCM. Also, DCMC was reacted with succinic dihydrazide (SDH) through Schiff's base reaction to give CMCSH. The water uptake of the prepared samples was also studied. All the modifications and reactions were confirmed by Fourier Transform Infrared Spectroscopy (FTIR), Scanning Electron Microscopy (SEM) and Transmission Electron Microscopy (TEM). Silver nanoparticles (AgNPs) were loaded onto the prepared cross-linked compounds and their loading was confirmed by EDX. The antimicrobial activities of the silver-loaded cross-linked compounds were investigated against gram-positive and gram-negative bacteria, as well as against yeasts.

**Keywords:** carboxymethyl cellulose, carboxymethyl hydrazide, Schiff's base, antimicrobial activity

### INTRODUCTION

Many olive tree species are grown around the world either for oil production or for table olives. Large quantities of by-products remain after the oil extraction process and their utilization would be beneficial for environmental reasons. At present, the wastes are generally used as fuel in factories. Because of the presence of polyphenolic compounds and oil residues, they are not recommended to be used as animal feed, unless treated.<sup>1</sup> Other chemical constituents of olive by-products include cellulose, hemicelluloses, lignin, carbohydrates, fats and free sugars.<sup>2</sup> Potential applications of such by-products include the production of activated carbon for water pollutant removal due to their accessibility and low cost.<sup>3,4</sup>

CMC has a great importance in the industry and everyday life. CMC is a linear, long chain, water soluble, anionic polysaccharide derived from cellulose. It is a white to cream colored, tasteless, odorless and water-soluble

polysaccharide with high molecular weight.<sup>5</sup> The utilization of CMC presents the advantages of non-toxicity, biocompatibility and biodegradability. It has various applications in fields such as textile industry, paper industry, detergents, pharmaceuticals, food industry and ceramics. Due to its various applications, CMC is produced in much higher amounts than any other cellulose derivative. Recently, the industrial importance of CMC has stimulated research attention towards the possibility of novel applications to replace synthesized polymers with natural ones. The modification of CMC is required to improve its chemical and physical properties.<sup>6</sup> CMC has been subjected to selective oxidation by using sodium metaperiodate, which breaks down the C<sub>2</sub>-C<sub>3</sub> bond in the glucose unit, resulting in dialdehyde (DCMC).<sup>7</sup> Also, CMC can be modified into a new carboxymethyl cellulose hydrazide (NCCM) by the reaction with



acetic acid. The product was collected after filtration and washed three times with 70% (w/w) aqueous ethanol, then the product was dried at 110 °C in an oven.

#### Degree of substitution

The DS of CMC is defined as the average number of carboxymethyl groups per repeating unit. CMC was firstly purified, and then the DS of the purified sample was determined as described below.

#### Purity of carboxymethyl

Exactly 0.5 g of carboxymethylated product was dissolved with 10 mL of water and stirred. Then, 10 mL of 1M hydrochloric acid was added and the mixture was agitated for complete dissolution. Five drops of phenolphthalein indicator were added into the mixture and then 1M sodium hydroxide was added dropwise under stirring until the solution turned red. Ethanol (50 mL, 95%) was slowly added into the mixture under stirring. Then, 100 mL of 95% ethanol was added and the mixture was left to settle for 15 min. After the solution had settled, the supernatant liquid was filtered by G3 type glass and discarded. The precipitate was washed four times with 80% ethanol and then washed again with 50 mL of 95% ethanol. The precipitate was dried in the oven at 105 °C for 4 h.

#### Determination of DS

The average values of degree of substitution (DS) were determined by acidometric titration. Exactly 0.2 g of carboxymethyl cellulose was weighed in a 250 mL flask and then 50 mL distilled water was added and stirred for 10 min. The pH value of the solution was adjusted up to 8 by adding acid or alkali. Then, the solution was titrated with 0.05M H<sub>2</sub>SO<sub>4</sub> until the pH of the solution decreased to 3.74, as determined by an acidometer.

The degree of substitution was calculated based on the equations:

$$A = m_o / m \quad (1)$$

$$B = 2 \times M \times V / a \times m \quad (2)$$

$$DS = 0.132 \times B / (1 - 0.08) \times B \quad (3)$$

where a is the purity of carboxymethyl hemicelluloses; m<sub>o</sub> and m are the carboxymethylated products after and before purification, M is the normality of the H<sub>2</sub>SO<sub>4</sub> used, V is the volume (mL) of the H<sub>2</sub>SO<sub>4</sub> used to titrate the sample, B is the mmol/g of the H<sub>2</sub>SO<sub>4</sub> consumed per gram of carboxymethylated products.

#### Oxidation of CMC

CMC was oxidized as previously described.<sup>16</sup> Briefly, 2 g CMCNa was dissolved in 20 mL deionized water and stirred to get a clear solution. 2 g sodium periodate was added to the CMC solution. The pH was adjusted to 3.0 with 1M sulfuric acid under stirring. The mixture was stirred at room temperature in the darkness for 24 h. Excess ethylene glycol was used to

decompose the remaining periodate and quench the reaction, while the oxidized product, referred to as dialdehyde carboxymethyl cellulose (DCMC), was precipitated by pouring the suspension into a large amount of ethanol and dried in the oven at 105 °C.

The degree of CMC oxidization was evaluated by the determination of the aldehyde content.<sup>17</sup> The oxidized CMC was converted to oxime by Schiff's base reaction with hydroxylamine hydrochloride. In detail, the procedure was as follows: about 0.5 g DCMC was dissolved in 25 mL distilled water and the pH was adjusted to 5 with NaOH. Then, 20 mL of 0.72 mol/L hydroxylamine hydrochloride in a pH 5 solution was added into the oxidized CMC solution. The mixture was stirred for 24 h, which was followed by the titration of the released hydrochloric acid with 1.0 mol/L NaOH. Here, the consumption of NaOH solution in liters was recorded as V<sub>c</sub>. The same concentration of the CMC solution at pH 5 was used as a blank and its consumption of the alkali solution in liters was recorded as V<sub>b</sub>. Thus, the aldehyde content in DCMC can be calculated by the following equation: Aldehyde content, % = 100 X ((V<sub>c</sub>-V<sub>b</sub>) x C<sub>NaOH</sub>) / 8 x m/M) (4) where C<sub>NaOH</sub> = 1.0 mol/L, m is the dry weight (g) of the DCMC sample and M is the molecular weight of the repeating unit of DCMC (approximately = 211 g/mol). The aldehyde content was found to be 40%.

#### Preparation of carboxymethyl hydrazide (NMC)

NMC was prepared by adding 0.09 mol of hydrazine monohydrate to 1 g CMC and 40 mL deionized water in a round-bottom flask, which was heated under reflux for 8 h. The separated solid was filtered, washed with methanol and dried at 45 °C.<sup>13</sup>

#### Preparation of succinic dihydrazide (SDH)

SDH was prepared by adding 0.09 mol of hydrazine monohydrate to 5 g succinic acid and 40 mL ethanol in a round-bottom flask, and was heated under reflux for 8 h. The separated solid was filtered, washed with methanol and dried at 45 °C (Scheme 2).<sup>13</sup> The structure of SDH was confirmed by FTIR, which indicated the introduction of the dihydrazide group into succinic acid.<sup>18</sup>

#### Reaction of DCMC with NMC

In a separate phosphate buffer solution (0.1 M pH 5.3-8.04), DCMC and NMC were dissolved, and stirred at 60 °C for 2 h. After that, the product DCMC/NMC was poured into a Petri dish and dried at 45 °C.<sup>19</sup>

#### Reaction of DCMC with SDH

2.06 mol of DCMC, 1.00 g CMC and (0.68, 2.05, 3.4, 4.79) mol of SDH were mixed and stirred for 2 h at 60 °C. Then the product DCMC/SDH was poured into a Petri dish and dried at 45 °C.<sup>19</sup>

**Loading and release of silver nanoparticles (AgNPs)**

AgNPs were loaded onto the reaction products of DCMC/NCMC and DCMC/SDH with NCMC and SDH. Silver release from AgNPs loaded DCMC/NCMC and DCMC/SDH was detected as follows: 1.0 g of AgNPs loaded substance was immersed into 10 mL deionized water for different time intervals, ranging from 1 to 24 h, at ambient temperature. The immersed sample was separated from the deionized water and a certain volume of the deionized water, including AgNPs, was drawn for analysis by atomic absorption (Agilent Technologies, 200 Sevia AA). The results represent the average of four measurements.<sup>20</sup>

Mmole of AgNPs release, % = 100 x (mmole AgNPs release/mmole of loaded AgNPs in test sample) (5)

**Characterization****Fourier Transform Infrared Spectroscopy**

The formed DCMC/NCMC and DCMC/SDH were calibrated using a Jasco Fourier Transform Infrared spectrometer (FT/IR-6100). To obtain the spectra, a pellet was made from the sample and KBr. Transmission was measured in the wavenumber range of 800-4400 cm<sup>-1</sup>.

**Morphological properties**

The morphology of the formed DCMC/NCMC and DCMC/SDH was observed using a Scanning Electron Microscope (SEM) (Hitachi High Technologies America, Schaumburg, IL) and a Transmission Electron Microscope (TEM). The samples to be observed under SEM were mounted on conductive adhesive tape and coated with gold palladium. The widths of the single cells obtained by maceration were measured from the SEM pictures and the lengths of the single cells were measured using a digital microscope.

**Elemental analysis**

The microanalysis of carbon, hydrogen and nitrogen was carried out using a Perkin-Elmer 2408 CHN analyzer at the Micro Analytical Center (National Research Center, Egypt).

**Gel fraction**

Normally, the hydrogel content of a given material is estimated by measuring its insoluble part in the dried sample after immersion into deionized water for 24 h at room temperature. The obtained DCMC/NCMC and DCMC/SDH were dried in a vacuum oven for 24 h and weighed ( $W_i$ ), then they were soaked in distilled water for 24 h. The samples were then dried in a vacuum oven and weighed again ( $W_d$ ). The gel fraction was then measured as follows:

Gel fraction, % = 100 x  $W_d/W_i$  (6)

**Water uptake**

The progress of the water uptake process was monitored gravimetrically, as described by other

researchers.<sup>21</sup> In a typical experiment, a preweighed piece of DCMC/NCMC and DCMC/SDH (1 g) was immersed in an aqueous reservoir using distilled water (pH 7.2) and allowed to swell for a definite time period. The swollen piece was taken out at predetermined time, pressed in between two filter paper sheets to remove excess water and weighed. The water uptake percentage can be determined as a function of time as follows:<sup>22</sup>

Water uptake, % = 100 x (( $m_t - m_0$ )/ $m_0$ ) (7)

where  $m_t$  is the weight of the swollen hydrogel sample at time  $t$  and  $m_0$  is the weight of the dry hydrogel sample.

**Antimicrobial assessments**

The agar plate method was used to evaluate the antimicrobial activities of the prepared hydrogels.<sup>23</sup> Three different test microbes: *Staphylococcus aureus* ATCC 6538, *Pseudomonas aeruginosa* ATCC 25416 and *Candida albicans* ATCC 1023, were selected as representatives of gram-positive, gram-negative bacteria and yeast species to evaluate the antimicrobial activities of the developed materials. The test microbes were grown on nutrient agar medium. The culture of each test microbe was diluted with sterilized distilled water to 10<sup>7</sup> to 10<sup>8</sup> colony forming units (CFU/mL), then 1 mL of each was used to inoculate a 1 L-Erlenmeyer flask, containing 250 mL of solidified agar medium.<sup>23</sup> The media were put onto previously sterilized Petri dishes (10 cm diameter, with 25 mL of solidified medium). DCMC/NCMC and DCMC/SDH discs (10 mm Ø) loaded with AgNPs were placed on the surface of the agar plates seeded with the test microbes and incubated for 24 h at the appropriate temperature for each test organism. The antimicrobial activities were recorded as the diameter of the clear zones (including the gel film itself) that appeared around the disks.

**RESULTS AND DISCUSSION****Oxidation of CMC**

Mild oxidation of the prepared CMC led to selective cleavage of the C<sub>2</sub>-C<sub>3</sub> bond in the pyranose ring of the cellulose chain, and to the conversion of two hydroxyl groups in positions 2, 3 into two aldehyde groups. The oxidation of CMC was elucidated by FTIR as shown in Figure 1, while particle size was measured by TEM as shown in Figure 2.

In the spectrum of DCMC (Fig. 1), its characteristic peak can be noted at 800 cm<sup>-1</sup>, which represents the hemiacetal bond between the aldehyde groups and the neighboring hydroxyl groups.<sup>18</sup> The peak at 3429 cm<sup>-1</sup> represents the OH in DCMC, compared with that at 3490 cm<sup>-1</sup> in the spectrum of CMC, the peak at 2800 cm<sup>-1</sup> represents the C-H stretching of aldehyde groups,

and that at  $1620\text{ cm}^{-1}$  belongs to the C=O of aldehyde.<sup>24</sup>

Figure 2 reveals that the particle size of DCMC appears in the nano-range, with an average particle size between 5.5-76.7 nm. Such particle size ensures a more rapid reaction and is in agreement with the results obtained by some other researchers.<sup>16</sup>

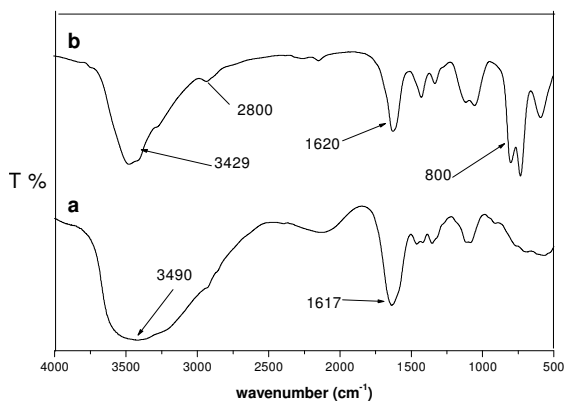
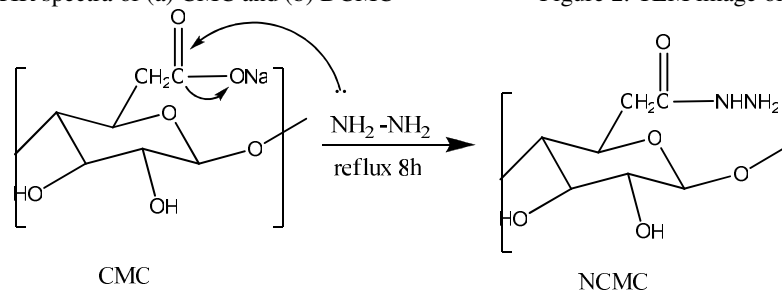


Figure 1: FTIR spectra of (a) CMC and (b) DCMC



Scheme 2: Preparation of NCMC

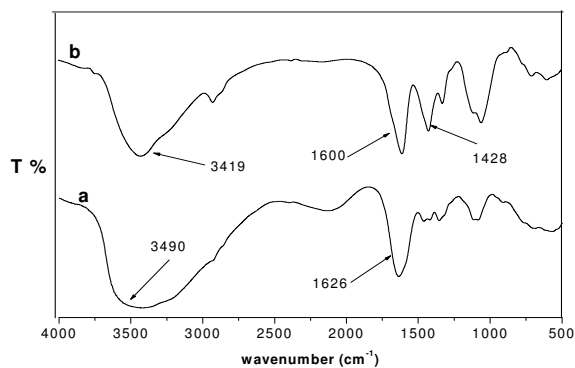


Figure 3: FTIR spectra of (a) CMC and (b) NCMC

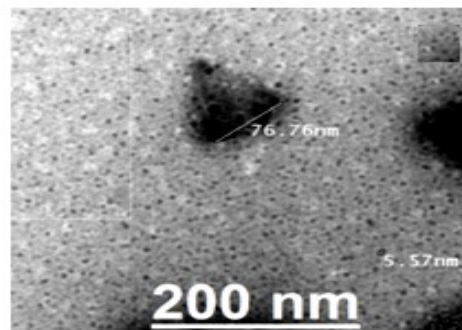


Figure 2: TEM image of DCMC

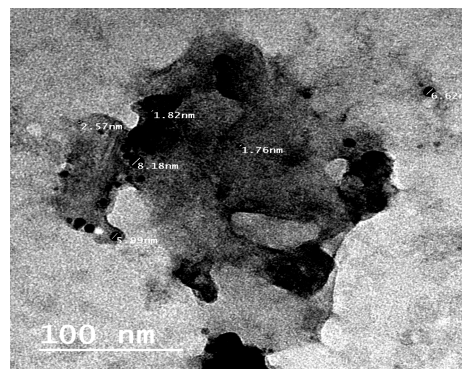
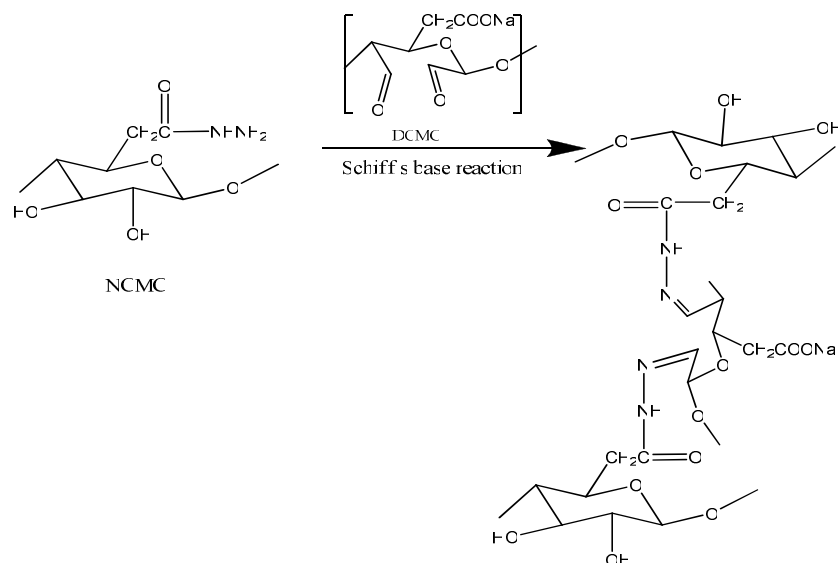


Figure 4: TEM image of NCMC



Scheme 3: Reaction of DCMC with NCMC

Hydrazide formation from CMC is illustrated by FTIR (Fig. 3). By comparing the spectra of CMC with NCMC, it may be remarked that the characteristic peaks at  $3400\text{ cm}^{-1}$ , due to OH in CMC, shifted to  $3419\text{ cm}^{-1}$  due to the presence of the  $\text{NH}_2$  group.<sup>7</sup> The band at  $1626\text{ cm}^{-1}$  belonging to C=O in CMC shifted to  $1600\text{ cm}^{-1}$  due to the C=O of the amide group in NCMC. Also, the band at  $1428\text{ cm}^{-1}$  appeared in the NCMC spectrum, representing C-N, which was also reported by other researchers.<sup>18</sup>

The particle size of NCMC was measured by TEM. Figure 4 reveals that the particle size of NCMC was in the nano-range (2-8 nm). Also, elemental analysis was used to describe different

elements in NCMC, which confirmed the presence of N, H and C in the ratio of 2.223, 8.08 and 33.41, respectively. The presence of C and H was expected, but the presence of N was due to hydrazide formation.

#### Reaction of DCMC with NCMC

The reaction between DCMC and NCMC is illustrated in Scheme 3. A Schiff's base reaction occurred between the amino group  $\text{NH}_2$  on NCMC and the aldehyde groups of DCMC.<sup>25</sup> DCMC was utilized to join two NCMC chains, forming a cross-linking product.<sup>16</sup> FTIR, SEM and elemental analysis confirmed the cross-linking.

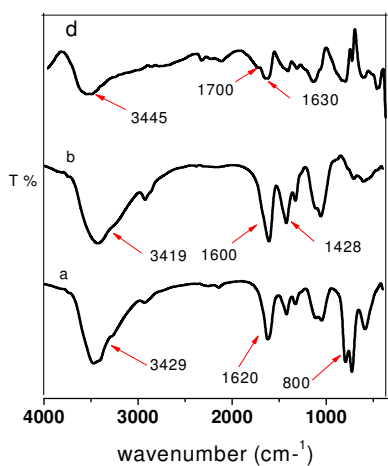


Figure 5: FTIR spectra of (a) DCMC, (b) NCMC and (c) DCMC/NCMC

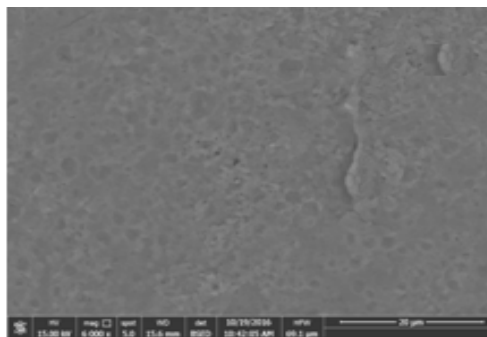


Figure 6: SEM image of DCMC/NCMC

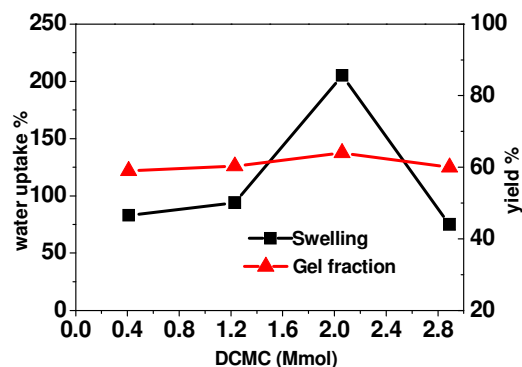


Figure 7: Effect of DCMC on water uptake and gel fraction

Figure 5 represents the FTIR spectrum of DCMC/NCMC, and those of DCMC and NCMC. In the spectrum of DCMC/NCMC, the peak at  $3545\text{ cm}^{-1}$  is due to OH and NH stretching. The peak at  $1700\text{ cm}^{-1}$  corresponds to the C=O of the amide linkage and it shifted to a higher value than in the spectra of each NCMC and DCMC. The characteristic peak at  $1630\text{ cm}^{-1}$  is due to the introduction of C=N in DCMC/NCMC.<sup>8</sup> In the spectra of DCMC, the peak at  $800\text{ cm}^{-1}$  belonging to hemiacetal disappeared because the C=O of DCMC was not available any more.

The morphological structure of DCMC/NCMC was studied by SEM and presented in Figure 6. The surface has a less porous appearance and is flat, but the entire structure has some holes. This structure affects the water uptake ability of the material.

Elemental analysis has been used to describe the changes in the element ratio of DCMC/NCMC. The ratios of N, H and C were 0.493, 1.62 and 18.44, respectively, which is less than those for pure NCMC.

The tendency of DCMC/NCMC to uptake water and its gel fraction were studied and reported in Figure 7. The water uptake ability was increased by increasing the amount of DCMC until the maximum value of 2.06 mmol of DCMC, and then decreased. This is possibly due to the increasing rate of cross-linking, as DCMC was converted to a hemiacetal configuration. This result is similar to that of some co-workers.<sup>26</sup>

### Preparation of SDH

Scheme 4 illustrates the condensation reaction pathway for the formation of SDH due to the reaction between succinic acid and hydrazine hydrate. The formed product SDH was studied by

FTIR, which indicated the introduction of the hydrazide group into succinic acid. The reaction occurred due to hydrazide substitution between -OH and  $\text{NH}_2$ .

Comparing the spectrum of pure succinic acid and that of SDH, it is remarked that the characteristic peak at  $3400\text{ cm}^{-1}$  due to  $\text{NH}_2$  appears in dihydrazide, while the peak at  $3000\text{ cm}^{-1}$  in succinic acid is due to OH.<sup>8</sup> The bands at  $1690\text{ cm}^{-1}$  and  $1413\text{ cm}^{-1}$  are due to C=O and COO symmetric stretch in succinic acid. The bands at  $1550$  and  $1403\text{ cm}^{-1}$  correspond to the amide group C=O and C-N in SDH.<sup>18</sup>

### Reaction of DCMC with SDH

As shown in Scheme 5, SDH reacts with DCMC through a Schiff's base reaction between the amino group of SDH and the aldehyde groups of DCMC.<sup>25</sup> SDH joins two DCMC chains forming a cross-linked product. FTIR, SEM and elemental analysis were used to confirm the cross-linking.

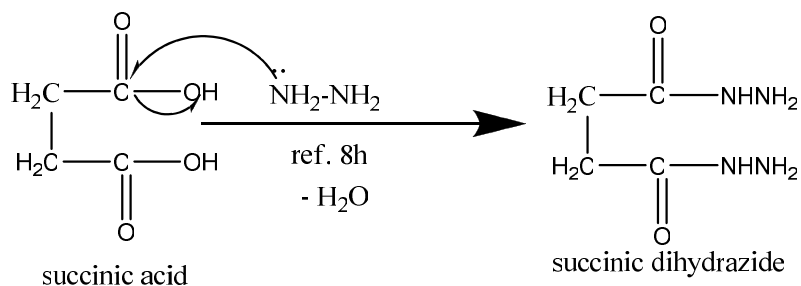
Figure 8 shows the FTIR spectrum of SDH as cross-linker. The peak at  $3425\text{ cm}^{-1}$  is due to OH and NH stretching. The peak at  $1650\text{ cm}^{-1}$  is shifted to a higher value than in the spectra of DCMC and SDH, due to the C=O of the amide linkage CONH. Also, the peak at  $1530\text{ cm}^{-1}$  is due to C=N amide linkage.<sup>5</sup> In the spectrum of DCMC, the peak at  $800\text{ cm}^{-1}$ , belonging to hemiacetal, disappeared.

Figure 9 illustrates the surface morphology of the cross-linked DCMC/SDH by the SEM technique. The surface has a lot of holes and appears as rough.

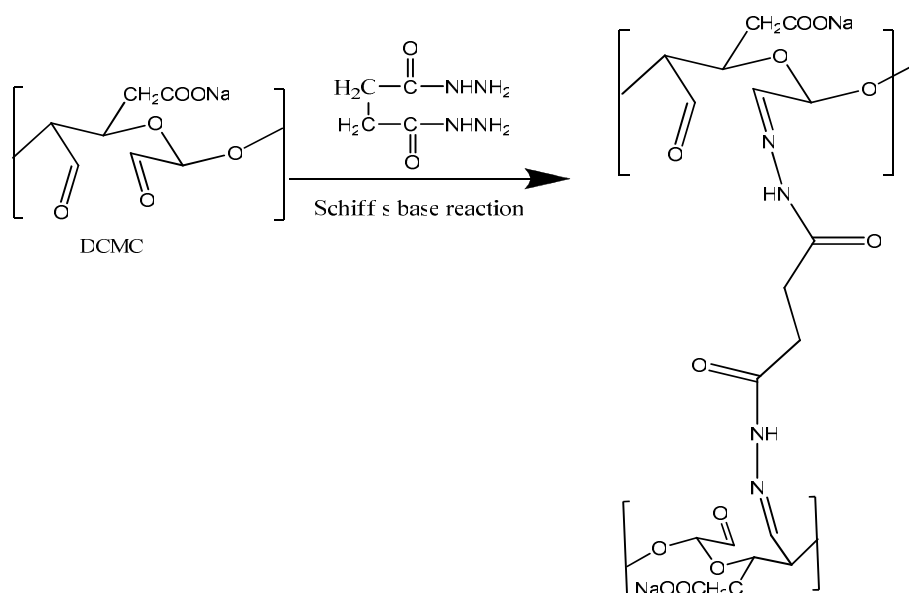
Figure 10 shows the ability of the cross-linked DCMC to uptake water, indicating a maximum at 0.68 mmol of SDH, followed by a decrease in the

water uptake percent. This trend may be explained by an increasing cross-linking density at higher cross-linker concentrations, resulting in

a rigid structure, which cannot be expanded and hold water.<sup>26</sup> This finding is similar to the results of other co-workers.<sup>27</sup>



Scheme 4: Succinic dihydrazide (SDH) formation



Scheme 5: Schiff's base reaction of DCMC with SDH

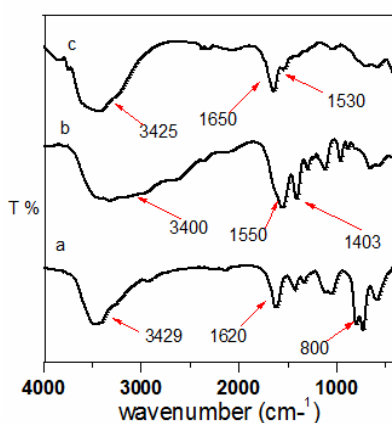


Figure 8: FTIR of (a) DCMC, (b) SDH and (c) cross-linked DCMC

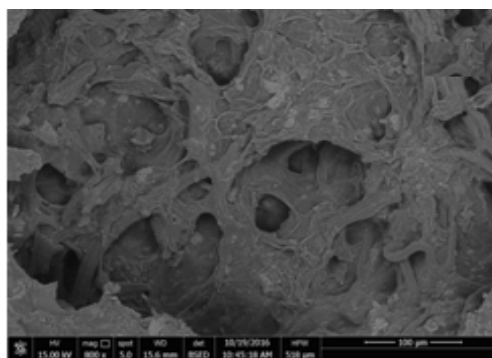


Figure 9: SEM image of cross-linked DCMC

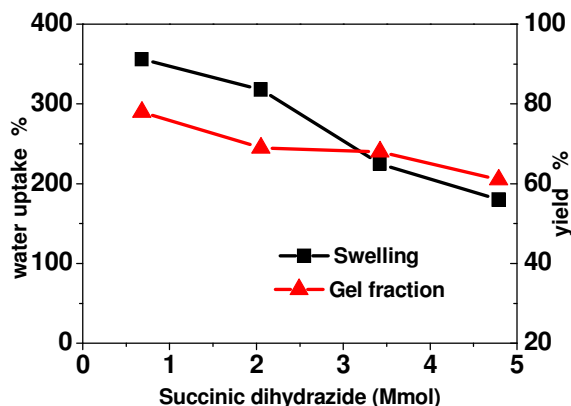


Figure 10: Effect of succinic dihydrazide on water uptake and yield

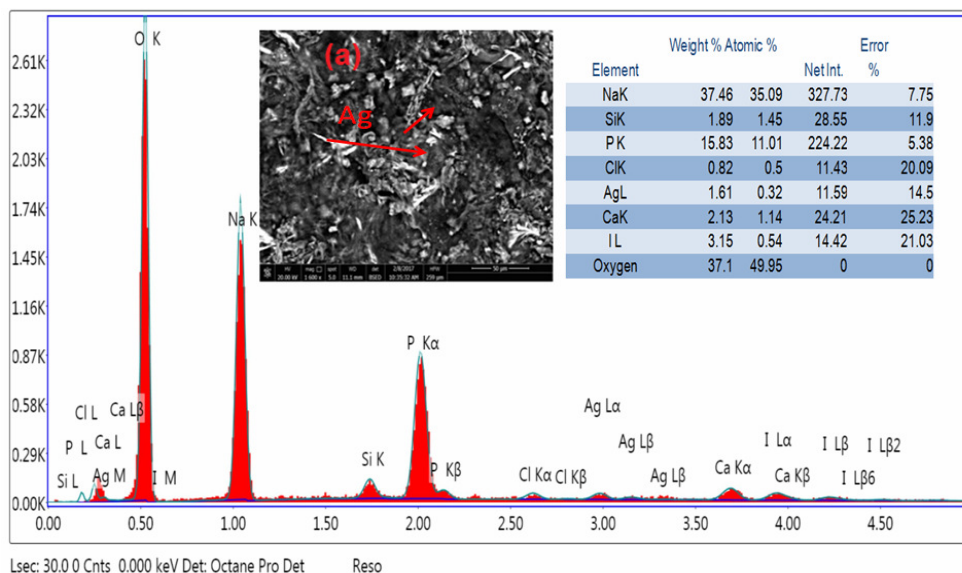
### Loading of AgNPs

The effect of AgNP loading on the water uptake of both cross-linked materials, as well as on the release of nanoparticles, was studied. The water uptake decreased with an increase in the amount of AgNPs, reaching 130 and 133% for cross-linked NCMC and DCMC, respectively. This may be explained by the fact that AgNPs penetrated through the cross-linked matrix, retarding water absorption, consequently, the water uptake decreased.<sup>28</sup>

Figure 11 illustrates the physical properties of both cross-linked NCMC and DCMC, as may be observed in the SEM images showing AgNP

distribution on the entire surface of both cross-linked materials. Silver appears as white particles on the entire surface. EDX analysis demonstrates the successful loading of AgNPs onto the cross-linked NCMC, which was higher than that onto the cross-linked DCMC.

Silver release from both cross-linked NCMC and DCMC is presented in Figure 12. AgNPs released rapidly at first, slowed down at 5 h and became constant after 24 h. It may be due to the presence of AgNPs in the structure of both cross-linked NCMC and DCMC as a result of a physical reaction, so when immersed into water the nanoparticles diffused rapidly.



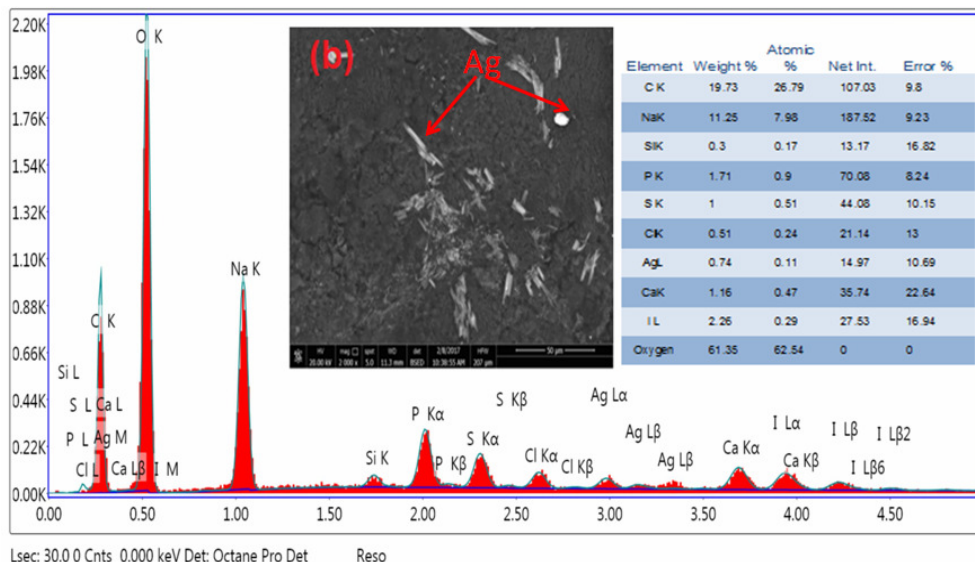


Figure 11: SEM and EDX of (a) cross-linked NCMC and (b) cross-linked DCMC

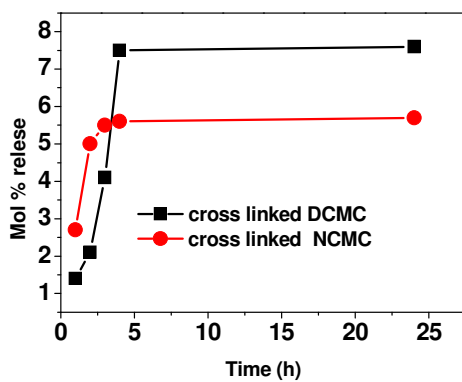


Figure 12: Release of AgNPs from both cross-linked NCMC and DCMC

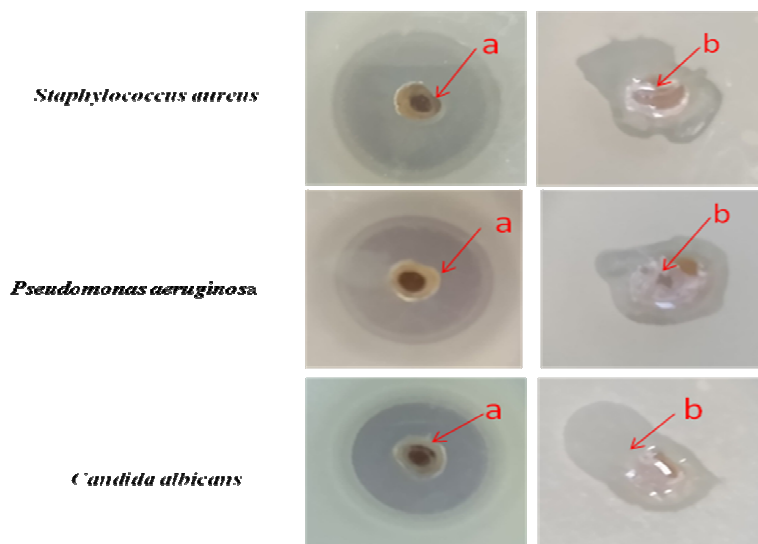


Figure 13: Antibacterial activities of cross-linked (a) NCMC and (b) DCMC loaded with AgNPs

### Antimicrobial activities

Figure 13 shows the effect of both cross-linked NCMC and DCMC loaded with AgNPs on gram-negative bacteria (*Pseudomonas aeruginosa*), gram-positive bacteria (*Staphylococcus aureus*), and the yeast *Candida albicans*. It has been found that the prepared cross-linked NCMC and DCMC containing AgNPs have antimicrobial properties, as demonstrated by the inhibition zones on the pictures. The effect of AgNPs on the microorganisms may be attributed to the formation of free radicals from the surface of Ag, which can attack the membrane and damage the cells of bacteria, leading to decomposition and destroying the membrane function.<sup>29</sup>

### CONCLUSION

A by-product of olive oil production was used to prepare value-added products, such as CMC, DCMC and NCMC. CMC was oxidized selectively by sodium periodate to form a dialdehyde derivative, which has high reaction efficiency. The formed product was confirmed by FTIR and TEM. CMC was modified to a new compound CMC-hydrazide, which was confirmed by FTIR. This compound was reacted with DCMC to form a cross-linked compound. The water uptake and gel fraction of the cross-linked compound were studied. Succinic dihydrazide was synthesized by the reaction of succinic acid and hydrazine monohydrate. DCMC was also cross-linked with succinic dihydrazide and the formed product was characterized by FTIR, EDX and SEM. AgNPs were loaded onto both of the formed cross-linked materials and the antimicrobial activity of the latter against *Staphylococcus aureus*, *Pseudomonas aeruginosa* and *Candida albicans* was demonstrated by the manifested inhibition zones.

### REFERENCES

- E. Molina and A. Nefzaoui, *Int. Biodeter. Biodegrad.*, **38**, 227 (1996), [https://doi.org/10.1016/S0964-8305\(96\)00055-8](https://doi.org/10.1016/S0964-8305(96)00055-8)
- R. Ghanbari, F. Anwar, K. M. Alkharfy, A. H. Gilani and N. Saari, *Int. J. Mol. Sci.*, **13**, 3291 (2012), doi: 10.3390/ijms13033291
- S. Kamel, H. Abou-Yousef *et al.*, *Carbohydr. Polym.*, **88**, 250 (2012), <https://doi.org/10.1016/j.carbpol.2011.11.090>
- K. Rouibah, A. H. Meniai, M. T. Rouibah, L. Deffous and M. B. Lehocine, *J. Desal. Water Treat.*, **16**, 393 (2010), <http://www.deswater.com/16toc.pdf>
- S. Dacrory, H. Abou-Yousef, R. E. Abou-Zeid, S. Kamel, M. S. Abdel-Aziz *et al.*, *J. Renew. Mater.*, **6**, 536 (2018), doi:10.7569/JRM.2017.634190
- S. Ahmed, M. El-Sakhawy and S. Kamel, *Int. J. Biol. Macromol.*, **93**, 1647 (2016), <https://doi.org/10.1016/j.ijbiomac.2016.04.029>
- L. Hongli, M. Changdao, B. Wu and W. Li, *Carbohydr. Polym.*, **84**, 881 (2011), <https://doi.org/10.1016/j.carbpol.2010.12.026>
- M. Nasim and N. M. Peyman, *Colloid. Polym. Sci.*, **294**, 199 (2016), <https://doi.org/10.1007/s00396-015-3768-4>
- P. Bulpitt and D. Aeschlimann, *J. Biomed. Mater. Res.*, **47**, 152 (1999), [https://doi.org/10.1002/\(SICI\)1097-4636\(199911\)47:2<152::AID-JBM5>3.0.CO;2-I](https://doi.org/10.1002/(SICI)1097-4636(199911)47:2<152::AID-JBM5>3.0.CO;2-I)
- A. Khademhosseini, G. Eng, J. Yeh, J. Fukuda, J. Blumling *et al.*, *J. Biomed. Mater. Res.*, **79**, 522 (2006), DOI:10.1002/jbm.a.30821
- U. J. Kim, S. Kuga, M. Wada, T. Okano and T. Kondo, *J. Biomacromol.*, **1**, 488 (2000), <https://doi.org/10.1021/bm0000337>
- C. D. Mu, F. Liu, Q. S. Cheng, H. L. Li, B. Wu *et al.*, *J. Macromol. Mater. Eng.*, **295**, 100 (2010).
- A. Tarek, A. Hatem, K. Adnan, B. Ahmed, T. Ahmad *et al.*, *Molecules*, **16**, 3544 (2011), <https://doi.org/10.3390/molecules16053544>
- S. Dacrory, H. Abou-Yousef, S. Kamel, R. E. Abou-Zeid, *Int. J. Biol. Macromol.*, **117**, 179 (2018), doi: 10.1016/j.ijbiomac.2018.05
- C. M. Y. Huang, P. X. Chia, C. S. S. Lim, J. Q. Nai, D. Y. Ding *et al.*, *Cellulose Chem. Technol.*, **51**, 665 (2017), [http://www.cellulosechemtechnol.ro/pdf/CCT7-8\(2017\)p.665-672.pdf](http://www.cellulosechemtechnol.ro/pdf/CCT7-8(2017)p.665-672.pdf)
- G. Jimin, G. Liming, L. Xinying, M. Changdao and L. Defu, *Food Hydrocol.*, **39**, 243 (2014), <https://doi.org/10.1016/j.foodhyd.2014.01.026>
- H. Li, B. Wu, C. Mu and W. Lin, *Carbohydr. Polym.*, **84**, 881 (2011), <https://doi.org/10.1016/j.carbpol.2010.12.026>
- L. Caicai, W. Xiaojuan, W. Guolin, W. Jingjing, W. Yinong *et al.*, *J. Biomed. Mater. Res. Part A*, **102**, 628 (2014), <https://doi.org/10.1002/jbm.a.34725>
- M. Changdao, L. Wei and L. Defu, *Food Hydrocol.*, **27**, 22 (2012), <https://doi.org/10.1016/j.foodhyd.2011.09.005>
- M.-V. Lungu, E. Vasile, M. Lucaci, D. Pătroi, N. Mihăilescu *et al.*, *Mater. Charact.*, **120**, 69 (2016), <https://doi.org/10.1016/j.matchar.2016.08.022>
- L. F. Gudeman and N. A. Peppas, *J. Appl. Polym. Sci.*, **55**, 919 (1995), <https://doi.org/10.1002/app.1995.070550610>
- A. Kostic, B. Adnadjevic, A. Bopovic and J. Jovanovic, *J. Serb. Chem. Soc.*, **72**, 1139 (2007).
- A. M. Youssef, S. A. Mohamed, M. S. Abdel-Aziz, M. E. Abdel-Aziz, G. Turkey *et al.*, *Carbohydr. Polym.*, **147**, 333 (2016), <https://doi.org/10.1016/j.carbpol.2016.03.085>

<sup>21</sup> D. Bruneel and E. Schacht, *Polymer*, **34**, 2628 (1993), [https://doi.org/10.1016/0032-3861\(93\)90600-F](https://doi.org/10.1016/0032-3861(93)90600-F)  
S. Dawlee, A. Sugandhi, B. Balakrishnan, D. Labarre and A. Jayakrishnan, *Biomacromol.*, **6**, 2040 (2005), DOI:10.1021/bm050013a

<sup>22</sup> J. Dahlmann, A. Krause, L. Möller, G. Kensah, M. Möwes *et al.*, *Int. J. Biomater.*, **34**, 940 (2013), doi: 10.1016/j.biomaterials.2012.10.008

<sup>23</sup> M. Sadeghi, F. Soleimani and M. Yarahmadi, *Oriental J. Chem.*, **27**, 967 (2011),

<http://www.orientjchem.org/vol27no3/chemical-modification-of-carboxymethyl-cellulose-via-graft-copolymerization-and-determination-of-the-grafting-parameters/>

<sup>24</sup> H. Abou-Yousef and S. Kamel, *J. Appl. Polym. Sci.*, **132**, 42327 (2015), <https://doi.org/10.1002/app.42327>

<sup>25</sup> H. Abou-Yousef, E. Saber, M. S. Abdel-Aziz and S. Kamel, *J. Soft Mater.*, **16**, 1 (2018), <https://doi.org/10.1080/1539445X.2018.1457540>